

DMRG study of the Bond Alternating $S=1/2$ Heisenberg ladder with Ferro-Antiferromagnetic couplings

J. Almeida*, M.A. Martin-Delgado* and G. Sierra*

**Departamento de Física Teórica I, Universidad Complutense. 28040 Madrid, Spain.*

**Instituto de Física Teórica, C.S.I.C.- U.A.M., Madrid, Spain.*

We obtain the phase diagram in the parameter space $(J'/J, \gamma)$ and an accurate estimate of the critical line separating the different phases. We show several measurements of the magnetization, dimerization, nearest neighbours correlation, and density of energy in the different zones of the phase diagram, as well as a measurement of the string order parameter proposed as the non vanishing phase order parameter characterizing Haldane phases. All these results will be compared in the limit $J'/J \gg 1$ with the behaviour of the $S = 1$ Bond Alternated Heisenberg Chain (BAHC). The analysis of our data supports the existence of a dimer phase separated by a critical line from a Haldane one, which has exactly the same nature as the Haldane phase in the $S = 1$ BAHC.

PACS numbers: 75.10.Jm 75.10.-b 74.20.Mn

I. INTRODUCTION

Quantum systems when placed in low dimensional lattices typically exhibit strongly correlated effects driving them towards regimes with no classical analog. Many properties of these regimes or quantum phases [1] depend in turn on the properties of their ground state and low lying energy excitations [2].

A problem of particular interest in the field of strongly correlated systems is the emergence of critical phases in a system where the generic behaviour as coupling constants are varied is to be a gapped system, although those gapped phases may be of different nature. In this paper we address this problem by selecting a system of quantum spins that allows us to perform a detailed study of critical and non-critical phases on equal footing, i.e., without any bias towards an a priori preferred phase. For reasons explained in Sect.II, the quantum spins are arranged in a 2-leg ladder lattice [3] with anti-ferromagnetic Heisenberg couplings along the legs while rung couplings are ferromagnetic. In addition, we also introduce an explicit dimerization coupling in the Hamiltonian along the leg directions, which can be varied from zero to strong values. This coupling plays a major role in order to create the aforementioned critical phases out of a system with only gapped phases.

This particular type of 2-leg ladder system has a number of open problems such as the precise location of critical phases in the phase diagram of the coupling constants, and the nature of the gapped phases it exhibits. Our study is complete enough so as to be able to solve for these problems in a very precise manner.

The understanding of these purely quantum effects is usually a hard problem. Perturbative and variational methods in quasi-one dimensional systems like chains and ladders are not well suited to uncover the physics in the whole range of coupling constants involved in the description of the interactions in the system. On the contrary the DMRG method [4], [5], [6], [7], [8] allows us to identify the critical phases clearly and without any bias. This

is so because the method is non-perturbative and allows a controllable management of errors.

Our studies are also of interest since experiments on ladder materials have revealed a very complex behaviour, such as an interplay between a spin-gapped normal states and superconductivity [9]. Moreover, a new field of study for these complex effects has been opened by the simulation of strongly correlated systems in optical lattices [10], in particular quantum spin chains and ladders [11].

This paper is organized as follows: in Sect.II we introduce the model Hamiltonian (1) describing a 2-leg ladder lattice of spins $S = \frac{1}{2}$ with columnar bond-alternating antiferromagnetic couplings in the horizontal direction and ferromagnetic couplings in the vertical direction, see Fig.1. We can identify some particular behaviours in appropriate weak and strong coupling limits, but not for generic values of the couplings. In Sect.III we point out the rich physical effects posed by open boundary conditions in these 2-leg ladders with finite length, although it also implies an a priori analysis in order to find out which low-lying states contribute to the gap of the system in the thermodynamic limit. This we can be done with the DMRG method by targeting several states and measuring their magnetization properties in the bulk and at the ends. Then, we compute numerically the gap and we establish the existence of a critical line in the quantum phase diagram of the model. A numerical fit of this critical curve is also given. In Sect.IV we determine the structure of the phase diagram by identifying the type of gapped phases occurring at each side of the critical line found in the previous section. They correspond to Haldane and dimer phases. They are identified by measuring the string order parameter and the dimerization parameter with the DMRG method. We complete our study of these phases measuring different observables. Sect.V is devoted to conclusions.

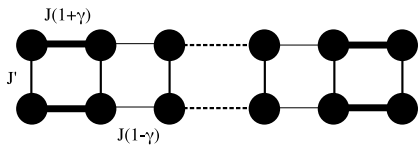


FIG. 1: Pictorial representation of the quantum Hamiltonian (1). The geometry of the lattice is a 2-leg ladder. Each solid dot is a spin $S = \frac{1}{2}$. In the horizontal direction (legs), we picture the bond alternation with strong links $J(1 + \gamma)$ and weak links $J(1 - \gamma)$. In the vertical direction (rungs), the system is arranged in the form of a columnar dimerization: strong links are parallel to one another, and similarly for weak links in the lattice.

II. THE MODEL

Competing ferromagnetic versus antiferromagnetic spin interactions may give rise to critical phases if they are appropriately arranged in certain quasi-one dimensional lattices. One emblematic example of this phenomenon is a lattice of quantum spins with the shape of a 2-leg ladder such that there are antiferromagnetic couplings along the legs and ferromagnetic interactions along the rungs connecting both legs. In addition, the antiferromagnetic couplings are bond-alternating in a columnar fashion. Dimerization interactions in the Hamiltonian are also known as staggered interactions. This configuration is shown in Fig.1. More precisely, this configuration of Heisenberg-like interactions is associated with the following quantum Hamiltonian

$$H = J \sum_{\ell=1,2} \sum_{i=1}^{L-1} (1 - (-1)^i \gamma) \mathbf{S}_i(\ell) \cdot \mathbf{S}_{i+1}(\ell) + J' \sum_{i=1}^L \mathbf{S}_i(1) \cdot \mathbf{S}_i(2), \quad (1)$$

where $\mathbf{S}_i(\ell)$ are quantum spin $S = \frac{1}{2}$ operators located at site i of the leg ℓ , and $J > 0$, $J' < 0$, $\gamma \in [-1, 1]$ are the antiferromagnetic, ferromagnetic and staggering couplings, respectively, as mentioned above.

Notice that several known regimes can be reached by tuning the coupling constants towards particular values. In the weak coupling limit, making $|J'/J| \ll 1$ we end up with a system consisting on two effectively decoupled $S = 1/2$ Heisenberg chains with bond alternation (BAHC), which are known to be gapped for every value of the dimerization parameter γ [12], except for the point $\gamma = 0$. In the strong coupling limit, making $|J'/J| \gg 1$, $J' < 0$ the system can be effectively described by a $S = 1$ spin chain with bond alternation, which is predicted to be gapped for all values of γ except for a critical point at a non-zero value γ_c [13]. These predictions are based on an approximate mapping onto the $O(3)$ σ model [14] at topological angle $\theta = 2\pi S(1 - \gamma)$. This yields a critical value of $\gamma_c = \frac{1}{2}$ when $\theta = \pi$, and

similarly another symmetric critical value at $\gamma_c = -\frac{1}{2}$. Thus, we shall always concentrate in the region $\gamma \geq 0$, due to the symmetry $\gamma \leftrightarrow -\gamma$ in the Hamiltonian (1). This non-linear sigma model (NL σ M) prediction misses the correct location of the critical point due to the approximations involved in that mapping. The exact location of this point has been widely studied [16] and results slightly varied depending on the approach, however modern studies place it at $\gamma_c = 0.259$ [15][17], also compatible with Fig.4(lower) which gives $\gamma_c = 0.2590 \pm 0.0001$ for a chain of 500 sites. These studies also conclude that the region $|\gamma| < \gamma_c$ corresponds to a Haldane phase while for $|\gamma| > \gamma_c$ we move to a dimer phase. The emergence of a dimerized $S = 1$ spin chain in the strong coupling limit can be explained by noting that as the rung coupling is ferromagnetic and strong $J' < 0$, $|J'| \gg J$, the two spins $S = \frac{1}{2}$ in each rung find energetically favorable to form a spin triplet.

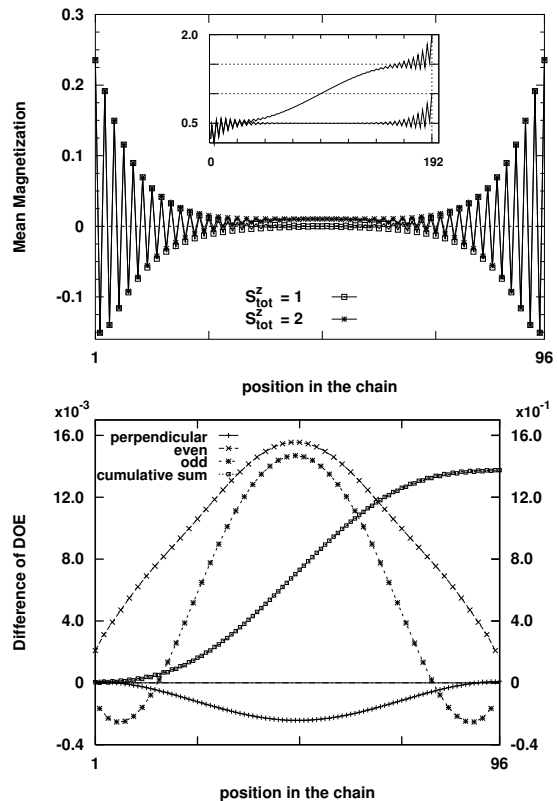


FIG. 2: Computations on a $L = 2 \times 96$ ladder at the point ($J'/J = -2.5, \gamma = 0$). *Up*: Mean magnetization $\langle S_i^z \rangle$ in the states with $S_{\text{tot}}^z = 1$ and $S_{\text{tot}}^z = 2$, as explained in the text. *Inset*: Cumulative sum of the magnetization over the whole extent of the ladder and the states with $S_{\text{tot}}^z = 1$ and $S_{\text{tot}}^z = 2$. The order of the sites in the x -axis corresponds in this case to the path used to traverse the ladder in a DMRG sweep. *Down*: Difference of energy density (DOE) of the excited states with $S_{\text{tot}}^z = 1$ and $S_{\text{tot}}^z = 2$: $\langle \mathbf{S}_{\ell,i} \mathbf{S}_{\ell',i'} \rangle_{S^z=2} - \langle \mathbf{S}_{\ell,i} \mathbf{S}_{\ell',i'} \rangle_{S^z=1}$. The scale on the right axis corresponds to the cumulative sum. See text for more explanations.

For generic values of the coupling constants in the

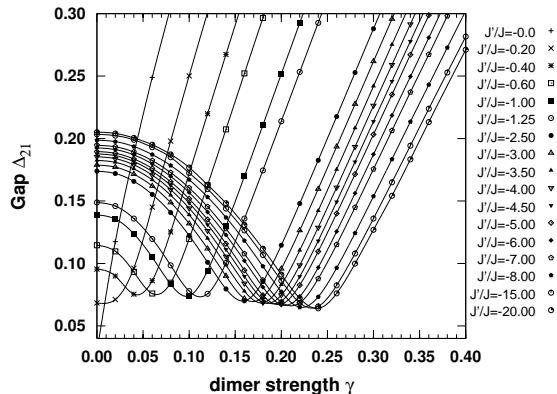


FIG. 3: Gap Δ_{21} computed on a $L = 2 \times 140$ ladder for different values of the parameter J'/J . Each minimum in the gap belongs to the critical line.

Hamiltonian (1), this model has been the subject of a series of conjectures based on exact diagonalization numerical studies [18] in the absence of dimerization $\gamma = 0$ and analytical studies using bosonization and NL σ M mapping [19] in the presence of dimerization $\gamma \neq 0$. Those numerical methods only allowed to reach ladder lengths typically of $L = 6$ or so, which prevents from reaching any definitive conclusion on the bulk properties of the system in the thermodynamic limit. As for the analytical studies, they conjectured the existence of a possible critical region, but due to the nature of the methods it is not possible to give its location in terms of the original coupling constants in the model Hamiltonian (1).

III. CRITICAL REGION

One of the main issues in this model (1) is whether it exhibits a critical line in the quantum phase diagram of J'/J vs. γ . We solve this open problem in the positive by using the DMRG method in finite version algorithm which provides us with better accuracy values than the infinite method version, although at the expense of more demanding time computing resources. The performance of the finite DMRG algorithm is characterized by the following parameters: the number of states m retained in the truncation process of the RG method, the weight of the discarded states w_m which is a measure of the DMRG error, the number of sweeps n_s or iterations of the method after the initial warm-up process and the tolerance ϵ of the target state energy which controls the average number of iterations that will need the diagonalization algorithm (Lanczos in our case) to compute the target state. We shall provide values of these parameters in our numerical computations below.

Before applying the finite-size DMRG method, two important remarks are in order:

i/ As we shall always work with a fixed value of L the length of the lattice, the gap $\Delta(J'/J, \gamma)$ is always finite

and only in the thermodynamic limit $L \rightarrow \infty$ it may vanish for certain values of J'/J and γ which define the critical line we are searching for. Thus, the signature of a gap in $\Delta(J'/J, \gamma)$ for fixed J'/J and varying γ will show up as a minimum in the dimerization parameter. Upon increasing the value of L , we shall obtain more robust estimations of the critical value $\gamma_c(J'/J)$ from the minima $\gamma_{\min}(L)$. This is a finite-size scaling analysis of the DMRG numerical data.

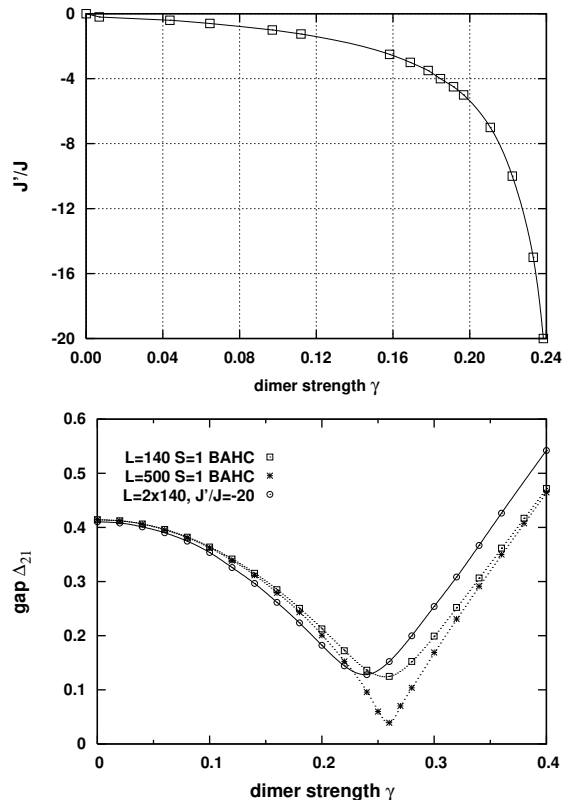


FIG. 4: *Top*: Critical region of a ladder of size $L = 2 \times 140$. The points of the critical line correspond to the coordinates that minimize $\Delta_{21}(\gamma, J'/J)$. The solid line is only a guide for the eye. *Bottom*: The value of the minimum gap for the ladder with $L = 2 \times 140$ sites is very similar to the corresponding $S = 1$ BAHC with $L = 140$ but the value of γ_c that minimizes this gap is still a bit shifted, which constitutes a signal that $J'/J = -20$ is still a low value to accurately mimic the limit BAHC behaviour. The computations for the $L = 500$ BAHC were performed storing $m = 450$ eigenvectors of the density matrix.

ii/ The physics of this 2-leg ladder (1) is richer when the lattice has open boundary conditions. Moreover, the numerical performance of the DMRG method is also better under these conditions. However, open boundary conditions must be handled with care in order to identify the gap $\Delta(J'/J, \gamma)$ we are after. We shall provide ways to do this identification by targeting appropriate low-lying states and measuring convenient observables with them.

In particular, using open boundary conditions we have found that the first excited state lies within the sector

with total z-spin angular momentum $S_{\text{tot}}^z = 1$, but in the Haldane phase it converges to the ground state that has $S_{\text{tot}}^z = 0$ as we take larger sizes of the system. We have then to consider the next excited state in the sector with $S_{\text{tot}}^z = 2$ to compute the gap of the spectrum as

$$\Delta_{21} := E_0(S_{\text{tot}}^z = 2) - E_0(S_{\text{tot}}^z = 1), \quad (2)$$

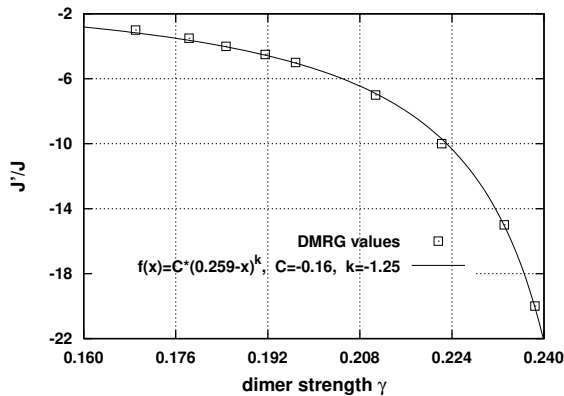


FIG. 5: The region of the critical line in the limit $|J'/J| \gg 1$ fits very well to a potential function of the form $J'/J = C(0.259 - \gamma_c)^k$, with $C = -0.16 \pm 0.01$ and $k = -1.25 \pm 0.01$.

The reason for considering Δ_{21} instead of $\Delta_{10} := E_0(S_{\text{tot}}^z = 1) - E_0(S_{\text{tot}}^z = 0)$ as the gap of the system, can be justified as follows: in the complete dimerized limit $\gamma = 1$, it is clear that the difference in energy between two arbitrary consecutive levels is the same, and corresponds exactly to the energy needed to promote one singlet bond to a triplet. The argument for the limit $\gamma = 0$ makes use of the properties of Haldane phases, where it is known to appear a non bulk excitation due to the existence of virtual spins at the end of the chain. Our conclusion is that the lowest lying state with $S_z^{\text{tot}} = 2$ consists on a superposition of two kind of excitations, namely the Haldane non-bulk triplet mentioned before and the bulk itself, also giving a triplet. Considering this scheme, in order to obtain the gap related to the bulk excitations we have to subtract the non bulk excitations present in the lowest lying states of sectors $S_z^{\text{tot}} = 1$ and $S_z^{\text{tot}} = 2$.

In Fig.2 we show rigorous comparisons of these two states in the Haldane limit $\gamma = 0$. Computations have been done on a $L = 2 \times 96$ ladder at the point $(J'/J = -2.5, \gamma = 0)$. On the *up* part of the figure, we plot the mean magnetization $\langle S_i^z \rangle$ in the states with $S_{\text{tot}}^z = 1$ and $S_{\text{tot}}^z = 2$, computed in one leg of the ladder, since due to the symmetry of the Hamiltonian, the magnetization is the same in both legs. As a check of the accuracy of our computations we observed that the results in both legs are the same up to the fifth or sixth decimal digit. In the *Inset* of that figure, we show the cumulative sum of the magnetization over the whole length of the ladder and the states with $S_{\text{tot}}^z = 1$ and $S_{\text{tot}}^z = 2$. The order of the sites in the x -axis corresponds in this case to the path used to traverse the ladder in a

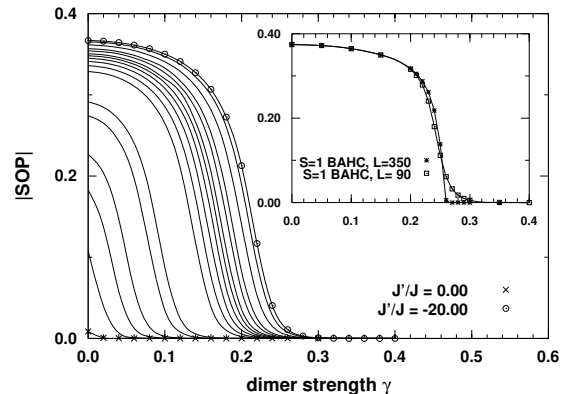


FIG. 6: String order parameter computed for a ladder consisting on $L = 2 \times 96$ sites. The SOP has been computed forming the triplets with adjacent $S = 1/2$ spins located in different legs. Clearly the value of this parameter is non-vanishing in the low region of γ , where the system is in the Haldane phase. The dimer phase is nonetheless characterized by a vanishing SOP. *Inset*: SOP computed for a $S = 1$ BAHC. The resemblance between both systems is evident in the region with $|J'/J| \gg 1$.

DMRG sweep. In the *down* part of this figure, we plot the difference of energy density of the excited states with $S_{\text{tot}}^z = 1$ and $S_{\text{tot}}^z = 2$: $\langle \mathbf{S}_{\ell,i} \mathbf{S}_{\ell',i'} \rangle_{S_z=2} - \langle \mathbf{S}_{\ell,i} \mathbf{S}_{\ell',i'} \rangle_{S_z=1}$. The difference has been divided into three contributions: the contribution labelled with *even* stands for links involving sites in the same leg and the even sublattice ($\ell' = \ell, i = 2k, i' = 2k + 1$), *odd* involves links joining sites in the same leg and the odd sublattice ($\ell' = \ell, i = 2k - 1, i' = 2k$), and *perpendicular* denotes links among legs ($\ell = 1, \ell' = 2, i = k, i' = k$). The cumulative sum of the difference of the various contribution, measured in the right axis scale, is also shown. Interestingly enough, we can observe the magnetization pattern at the ends being almost identical in the states with $S_{\text{tot}}^z = 1$ and $S_{\text{tot}}^z = 2$. The contribution to the z -axis projection of the spin coming from the ends is equal to 1 in both cases. Notice also that the difference of the density of energy between these states is close to zero at the ends, while it becomes clearly appreciable in the bulk. All these facts strongly support the picture of a non-bulk triplet excitation with the same nature in both states, that leaves the bulk of the chain with a neat value of the projection equal to $S_{\text{bulk}}^z = 0$ and $S_{\text{bulk}}^z = 1$ and gives a strong hint on the equivalence of Δ_{10} with periodic boundary conditions and Δ_{21} for open systems.

After this previous analysis to identify the states needed to target the gap of the system, we present in Fig.3 some values of the gap Δ_{21} for a ladder consisting on $L = 2 \times 140$ sites, at different regions of the parameter space. Computations have been performed retaining $m = 300$ states of the density matrix and the grid used to explore the phase diagram is $\gamma \in [0, 0.4]$, and $-J'/J = \{0.00, 0.20, 0.40, 0.60, 1.25, 2.50, 3.00, 3.50, 4.00, 4.50, 5.00, 6.00, 7.00, 10.00, 15.00, 20.00\}$. The existence of a set

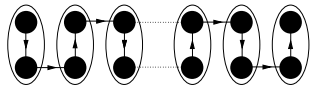


FIG. 7: A picture of the path used to compute the string order parameter in the 2-leg ladder with columnar bond alternation. The ellipses mean that the sites within them are forming a triplet.

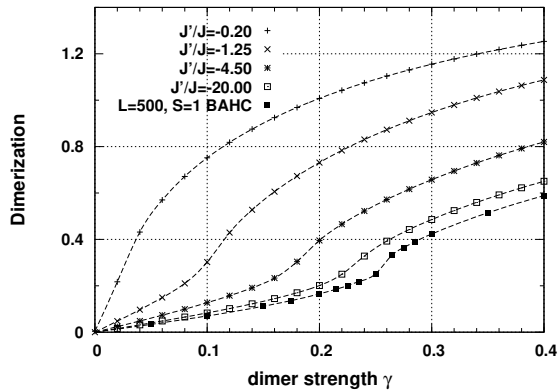


FIG. 8: Different values of the dimerization parameter $D_i := \sum_{\ell=1,2} \langle \mathbf{S}_{\ell,i-1} \mathbf{S}_{\ell,i} \rangle - \langle \mathbf{S}_{\ell,i} \mathbf{S}_{\ell,i+1} \rangle$ computed in the middle of a ladder of $L = 2 \times 96$ sites. Since we are explicitly introducing some staggering in the Hamiltonian (1), the dimerization parameter is non-vanishing even in the Haldane phase. However, the shape of the graphs seem to have an inflexion at the critical point. The graph corresponding to the $S = 1$ BAHC, has been scaled down by a factor 1/2 due to the effective coupling constant of the ladder, which is known to be half the constant corresponding to the BAHC.

of minima in the function $\Delta_{21}(\gamma, J'/J)$ is clear in this graph, although they shall become more distinguishable as we move to higher values of $|J'/J|$.

As an instance of the accuracy of our results, we point out that a systematic examination of the error in each of the truncations of our DMRG computations reveals that the highest values in the whole process are of the order of $w_m \sim 10^{-8}$, and mostly they are of order $w_m \sim 10^{-10}$. To obtain a suitable accuracy in the results we have set the number of sweeps $n_s = 2$ and the tolerance to $1e - 9$. To compute with enough precision the critical value $\gamma_c(J'/J)$ that minimizes the gap it becomes necessary to use large amount of data. On this regard, we have used interpolated values resulting from the DMRG computations.

Now, we can detect the presence of a critical line in the quantum phase diagram separating gapped phases. In Fig.4 we plot the critical region consisting of the coordinates for each minimum in Fig.3. In earlier studies [15], we placed the critical point of the $S = 1$ bond-alternating Heisenberg chain (BAHC) at $\gamma_c = 0.259$. The curve shown in Fig.4 shows a vertical asymptota that is still a bit off from this limiting value corresponding to

the region $|J'/J| \gg 1$, but this is simply because we have chosen a value of $J'/J = -20$ which is still not big enough and also due to finite-size effects on the 2-leg ladder. In the lower plots of Fig.4 we address these possibilities by comparing our ladder in the strong ferromagnetic limit with a pure $S = 1$ BAHCs with different sizes. Two parameters are important in this discussion, namely, the value $\gamma_c(J'/J)$ that minimizes the gap, and the value of the gap itself at this point $\Delta_{21}(\gamma_c)$. As we can observe in Fig.3, the value of $\Delta_{21}(\gamma_c)$ does not strongly depend on the particular choice of the coupling constant ratio J'/J , while it is definitely influenced by the size of the system. In Fig.4(lower) it is shown that the shift of γ_c computed for two $S = 1$ BAHCs with different sizes, but still large enough both, is less noticeable than the difference in their value of $\Delta_{21}(\gamma_c)$. It is clear the similarity of this magnitude in the case of the ladder and the corresponding BAHC, as well as the shift in the value of γ_c . All this make us conclude that in order to attain a better convergence with the $S = 1$ BAHC and a better estimate of the critical asymptota $\gamma_c = 0.259$, we shall increase the strength of the ferromagnetic coupling rather than the size of the system.

As we have a set of numerical data from the finite-size analysis of the critical line, we can also make a numerical estimation of the criticality curve. In fig. 5 we present a fit of the critical curve in the region close to $\gamma_c \simeq 0.259$. We choose as trial function for this fitting an inverse power law with some coefficients and exponents that are fixed by our numerics, namely,

$$J'/J = \frac{C}{(0.259 - \gamma)^k}. \quad (3)$$

The fitting yields the following estimations for the values of the parameters C and k that best fit the data: $C = -0.16 \pm 0.01$ and $k = 1.25 \pm 0.01$, and for simplicity the value of $\gamma_c = 0.259$ is taken for fixed.

IV. HALDANE AND DIMER PHASES

Once we have established the existence of a critical line in the quantum phase diagram of the model (1), it is natural to wonder about the two gapped phases that this line separates. More specifically, whether they are different or not and their identification as quantum phases in the framework of strongly correlated systems.

The possible nature of those phases can be guessed from the strong ferromagnetic limit $1 \ll |J'/J|$ of the ladder, effectively leading to the $S = 1$ BAHC. The phases of this chain are known to be the massive Haldane phase, separated by a critical point from the also massive dimer phase. To test the nature of each phase, we will resort to two different order parameters. The Haldane phase is known to exhibit a particular hidden order that can be measured by the string order parameter (SOP) [20], [21]. The definition of this operator for a spin-1 chain is

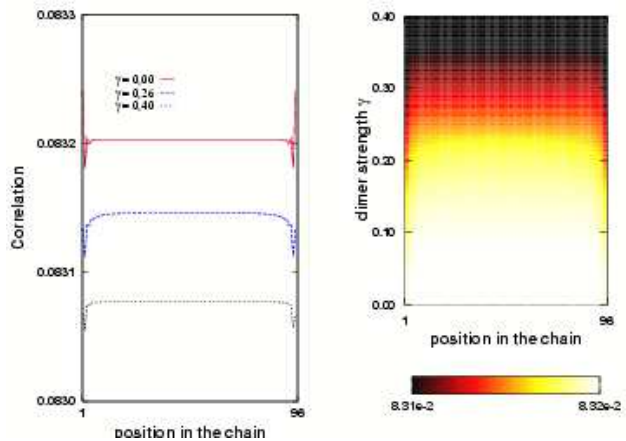


FIG. 9: Correlation $\langle S_i^z(1)S_i^z(2) \rangle$ in the ground state of a $L = 2 \times 96$ sites ladder and $J'/J = -20$. The plot on the left shows the correlation value for some arbitrary values of γ . The plot on the right shows the value of this magnitude in the whole region of the parameter γ .

as follows:

$$O(\ell) = \langle S_1^z \prod_{k=2}^{\ell-1} e^{i\pi S_k^z} S_\ell^z \rangle \quad (4)$$

This operator acting on our ground state measures how far it is from a spin liquid Néel state consisting on a sequence of $S = 1$ spins such that every spin with projection $S_i^z = \pm 1$ is followed by $S_{i+k}^z = \mp 1$ and $S_{i+k'}^z = 0$ for every $0 < k' < k$.

When we deal with $S = 1/2$ particles, to compute the SOP we have to define the pairs of particles which are most likely to couple to give a triplet and compute the SOP along the path connecting them. In our case, the existence of a ferromagnetic coupling clearly suggests that the triplets will result via this coupling. It is also worth recalling that the SOP is a parameter suited to work with translational invariant systems. In order to correctly estimate the SOP in open systems, we must restrict the computation to a region shorter than the whole length of the chain where end-effects are negligible and only bulk physics is relevant. In Fig.6 we show the SOP computed traversing the path shown in Fig.7. We can observe a non-vanishing SOP in the Haldane region, while it rapidly decays to zero in the dimer phase. The inset shows the SOP computed for a $S = 1$ BAHC and the resemblance between both systems is apparent.

Therefore, the phase below the critical line in the numerical phase diagram of Fig.4 is a gapped Haldane phase.

As for the region above the critical line in Fig.4, we have guessed from the strong coupling limit that it may be a dimer phase. The structure of a dimer phase is such that full translational invariance symmetry of the system is broken by one unit cell of the lattice. This situation can be detected by means of the dimerization parameter,

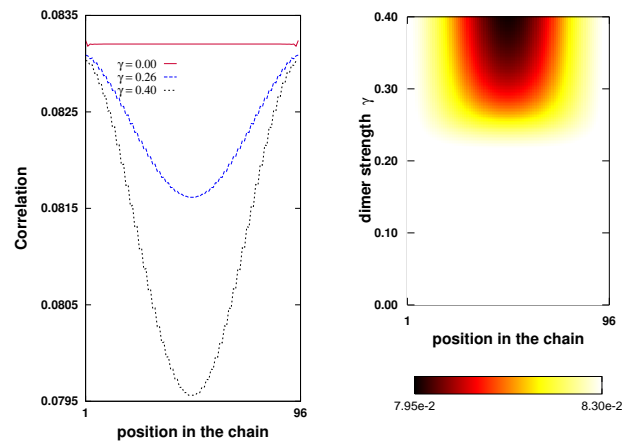


FIG. 10: Correlation $\langle S_i^z(1)S_i^z(2) \rangle$ in the first lying excited state in the sector with $S_{\text{tot}}^z = 1$ of a $L = 2 \times 96$ ladder and $J'/J = -20$.

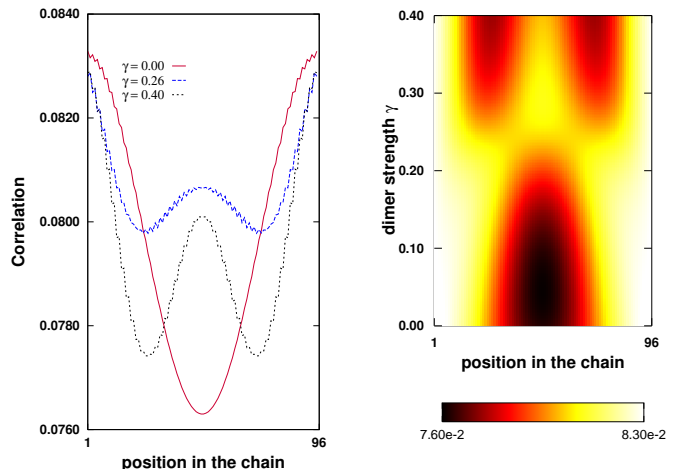


FIG. 11: Correlation $\langle S_i^z(1)S_i^z(2) \rangle$ in the first lying excited state in the sector with $S_{\text{tot}}^z = 2$ of a ladder consisting on $L = 2 \times 96$ sites and $J'/J = -20$.

which can be defined for our particular 2-leg ladder as

$$D_i := \sum_{\ell=1,2} \langle \mathbf{S}_{i-1}(\ell) \cdot \mathbf{S}_i(\ell) \rangle - \langle \mathbf{S}_i(\ell) \cdot \mathbf{S}_{i+1}(\ell) \rangle. \quad (5)$$

The subindex i is necessary since open systems are intrinsically not translationally invariant. In Fig.8 it is plotted the dimerization parameter of the ladder measured in the middle of the chain. Since staggering is explicitly introduced into the Hamiltonian (1), the order parameter vanishes only at $\gamma = 0$, but is finite even in the Haldane phase. Nevertheless, our plots clearly exhibit different behaviours related to the convexity of the parameter at each phase. This observation indicates that an accurate estimation of the point of inflexion in the dimerization parameter could be used as a measure of the critical point separating both phases.

We have also performed some measurements in the ladder to give more hints to understand the nature of

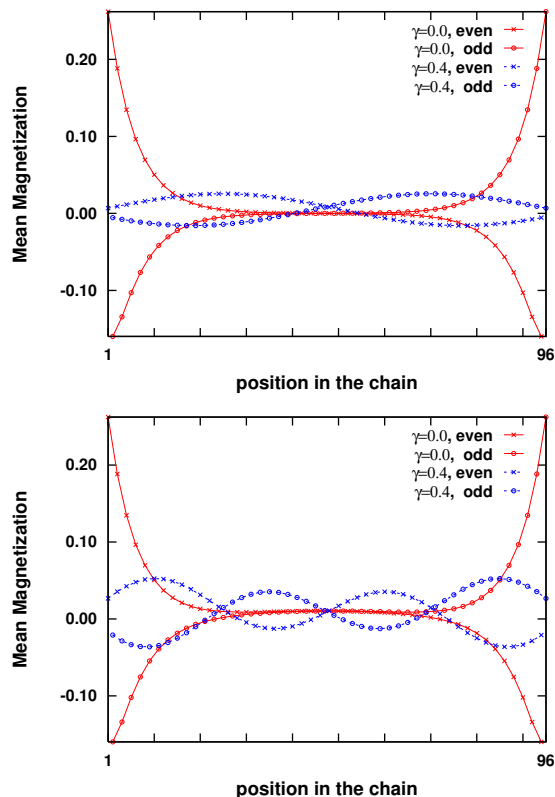


FIG. 12: Magnetization curves in a $L = 2 \times 96$ ladder for the lowest lying states in the sectors $S_{\text{tot}}^z = 1$ (top), and $S_{\text{tot}}^z = 2$ (bottom). The curves are separated in the different sublattices consisting on the sites occupying odd or even positions. Notice that both states present a peaked magnetization at the ends for $\gamma = 0.0$ well into the Haldane phase, while it vanishes in the dimer phase with $\gamma = 0.4$.

both phases. Figures 9, 10, and 11 show the correlation $\langle \mathbf{S}_i(1)\mathbf{S}_i(2) \rangle$ between sites in the perpendicular rungs. The pattern of the correlation can be understood by noticing that the correlation between two isolated $S = 1/2$ spins coupled to give a singlet is $\langle \mathbf{S}_1\mathbf{S}_2 \rangle / 3 = -1/4$ while it equals $1/12$ if the spins form a triplet. From these values we observe that the perpendicular rungs in the ground state are forming triplets and the distribution is uniform all along the ladder. In the excited states however, the triplet strength of some rungs is weakened, signaling the presence of magnon-like excitations, also

apparent in Fig.12. The nature of the non-bulk excitation present in the Haldane phase is not magnon-like and that explains the different number of kinks in the Haldane and dimer phase in Fig.10 and Fig.11.

V. CONCLUSIONS

We have determined the existence of a critical line in the quantum phase diagram of a 2-leg ladder with columnar dimerization and ferromagnetic vs. antiferromagnetic couplings. In this study, we use the finite-size system DMRG method which allows us to give the location of that critical curve. Moreover, we have clearly identified the two phases separated by the critical line to be a Haldane phase and a dimer phase. This identification is carried out by measuring the string order parameter and the dimerization order parameter in the whole range of values of the coupling constant ratio J'/J and dimerization parameter γ .

As a byproduct, we have introduced a systematic analysis of the spins at the borders of the open 2-leg ladder lattice. Our model is based on $S = \frac{1}{2}$ spins, then these end-chain spins exhibit physical effects of their own. They are real spins unlike the virtual spins appearing in integer spin chains or ladders. Their physics is specially interesting when the system size is finite, and even during the process of reaching the thermodynamic limit they produce non-trivial finite-size effects along the way. These facts difficult the technical analysis of the opening or closing of a gap in the low-lying spectrum of a 2-leg ladder with open boundary conditions. We have solved these difficulties by analyzing the ground state and low-lying energy excitations with respect to their bulk and boundary properties such as local magnetization and the like. With this information, it is possible to identify which states contribute to the gap in thermodynamic limit. These low-lying states have a definite total spin S^z and they can be targeted with the DMRG method. In this fashion, we have been able to identify the gapped or gapless behaviour of the model within the framework of the DMRG with open boundary conditions. *Acknowledgements* We acknowledge financial support from DGS grants under contracts BFM 2003-05316-C02-01, FIS2006-04885, and the ESF Science Programme INSTANS 2005-2010.

-
- [1] S. Sachdev, "Quantum Phase Transitions"; Cambridge University Press, (1999).
 [2] J. González, M.A. Martín-Delgado, G. Sierra, A.H. Vozmediano, *Quantum Electron Liquids and High- T_c Superconductivity*, Lecture Notes in Physics, Monographs vol. **38**. Springer-Verlag (1995).
 [3] E. Dagotto, T. M. Rice, "Surprises on the Way from One- to Two-Dimensional Quantum Magnets: The Lad-

- der Materials", *Science* **271** 618 - 623, (1996).
 [4] S.R. White, "Density-matrix algorithms for quantum renormalization groups" *Phys. Rev. B* **48**, 10345 (1993).
 [5] S. White, *Phys. Rev. B* **48**, 10345 (1993)
 [6] K. Hallberg, "New Trends in Density Matrix Renormalization"; *Adv.Phys.* **55** 477-526 (2006); cond-mat/0609039.
 [7] A. Schollwöck, *The density matrix renormalization*

- group, *Rev. Mod. Phys.*, **77**, 259 (2005).
- [8] *Density Matrix Renormalization*, edited by I. Peschel, X. Wang, M. Kaulke and K. Hallberg (Series: Lecture Notes in Physics, Springer, Berlin, 1999)
- [9] E. Dagotto, "Experiments on ladders reveal a complex interplay between a spin-gapped normal state and superconductivity",
- [10] M. Greiner, O. Mandel, T. Esslinger, Th. W. Hänsch, and I. Bloch, *Nature* **415**, 39 (2002); M. Greiner, O. Mandel, Th. W. Hänsch, and I. Bloch, *Nature* **419**, 51 (2002).
- [11] J. J. Garcia-Ripoll, M. A. Martin-Delgado, J. I. Cirac, "Implementation of Spin Hamiltonians in Optical Lattices"; *Phys. Rev. Lett.* **93**, 250405 (2004); cond-mat/0404566.
- [12] K. Hida, "Crossover between the Haldane-gap phase and the dimer phase in the spin-1/2 alternating Heisenberg chain", *Phys. Rev. B* **45**, 2207-2212 (1992).
- [13] I. Affleck, F. D. M. Haldane, "Critical theory of quantum spin chains"; *Phys. Rev. B* **36** (1987) 5291.
- [14] F. D. M. Haldane, "Continuum dynamics of the 1-D Heisenberg antiferromagnet: Identification with the O(3) nonlinear sigma model", *Phys. Lett. A* **93**, 464-468 (1982).
- [15] J. Almeida, M.A. Martin-Delgado, G. Sierra, "DMRG applied to critical systems: spin chains". XI Training Course on Strongly Correlated Systems. Salerno (Italy) October 2006.
- [16] K. Totsuka, Y. Nishiyama, N. Hatano, M. Suzuki, "Isotropic spin-1 chains with bond alternation: analytic and numerical studies", *Journal of Physics: Condensed Matter*, **7**, 4895-4920 (1995).
- [17] M. Kohno, M. Takahashi, M. Hagiwara, "Low-temperature properties of the spin-1 antiferromagnetic Heisenberg chain with bond alternation", *Physical Review B*, **57**, 1046-1051 (1998).
- [18] H. Watanabe, "Numerical diagonalization study of an S=1/2 ladder model with open boundary conditions"; *Phys. Rev. B* **50**, (13442-13448 1994).
- [19] K. Totsuka, M. Suzuki, "The spin-1/2 Heisenberg spin ladder with bond alternation", *Journal of Physics: Condensed Matter* **7** 6079-6096 (1995).
- [20] M. den Nijs, K. Rommelse, "Preroughening transitions in crystal surfaces and valence-bond phases in quantum spin chains", *Phys. Rev. B* **40**, 4709 (1989).
- [21] T. Kennedy, H. Tasaki, "Hidden $Z_2 \times Z_2$ symmetry breaking in Haldane-gap antiferromagnets", *Phys. Rev. B* **45**, 304 (1992).